

Recent developments in microwave filters based on GaN/Si SAW resonators, operating at frequencies above 5 GHz

Alina-Cristina Bunea⁽¹⁾, Dan Neculoiu⁽¹⁾, Adrian Dinescu⁽¹⁾, Leo Arij Farhat⁽²⁾

⁽¹⁾*National Institute of R&D in Microtechnologies (IMT) Bucharest, Romania*
Email: alina.bunea@imt.ro; dan.neculoiu@imt.ro; adrian.dinescu@imt.ro

⁽²⁾*ESTEC, ESA, Keplerlaan 1, Noordwijk, The Netherlands*
Email: leo.farhat@esa.int

I. INTRODUCTION

This communication presents the progress in the development of monolithic integrated band pass filters, achieved in the frame of the ESA project No. 40000115202/15/NL/CBi (“Microwave filters based on GaN/Si SAW resonators, operating at frequencies above 5 GHz”). The main objective focused on the design, fabrication and characterization of compact band pass filters processed on a 1 μm thin epitaxial GaN layer, grown on a silicon substrate, operating at ~ 5 GHz. In order to achieve this goal, inter-digital transducers (IDT) with digit/interdigit widths below 200 nm were designed. Due to the high losses occurring in the case of transversal filters, an approach based on the use of multiple Surface Acoustic Wave Resonators (SAW-Rs) was developed.

This approach requires an accurate control of the series and parallel resonance frequencies of the different SAW-Rs placed in series or in parallel with the signal path. Since it is difficult to tune the resonance frequencies by means of metallization thickness and/or digit/interdigit widths at the level of accuracy required by the filter design, the new approach uses printed inductors connected in series or in parallel with the SAW-R. At frequencies higher than 5 GHz, these inductors are in the 0.2 – 2 nH range and can be integrated monolithically into the SAW-R based filter structure, resulting in a very compact device.

Printed inductors connected in series and monolithically integrated with SAW-Rs with IDT digit/interdigit widths within the 130-200 nm range, operating in the 5.4 – 8.6 GHz frequency range, will be presented. It will be shown that series connected inductors with values between 0.2 – 1 nH tune the series resonant frequency of the SAW-R with up to 0.75%. An effective coupling coefficient of 1% was measured for these structures. The temperature effect on the tuned SAW resonators was investigated and the temperature coefficient of frequency is about -40 ppm/K.

Because of the high influence on the performance of the filter, the effect of the technological dispersion on the response of SAW-Rs fabricated on GaN/Si is studied. SAW-R test structures with interdigital transducers having the digit/interdigit widths of 200 nm were processed on a quarter of a 3 inch wafer and the resonant frequency deviation as a function of the position on the wafer is analyzed. The effects on the resonance frequency of the variation of the GaN layer thickness, the metallization thickness, the electrode width and the variation of the elastic constants due to the thermal strain are extracted from COMSOL simulations and compared to the expected deviation of the resonant frequency based on structural characterization results (SEM, AFM, ellipsometry).

The SAW band pass filter design with SAW-Rs controlled by series and parallel connected inductors is presented. It consists of three SAW-Rs connected in a PI-type configuration. The filter is optimized at circuit level, with a reasonable estimate of the mechanical, conductive and dielectric losses. The simulated insertion losses are about 10.4 dB at 5.5 GHz, the rejection is better than 40 dB at 5.42 GHz and 5.58 GHz. The 3 dB bandwidth is 8 MHz. The effect of a higher level of different losses on the transmission characteristics is also investigated.

II. SAW BAND PASS FILTER CONFIGURATIONS

Common SAW based band-pass filters (BPF) include: delay line type filters, longitudinally-coupled resonator filters and impedance element filters (ladder filters), schematically shown in Fig.1 (a), (b) and (c), respectively [1]. At frequencies higher than 5 GHz, since wire connections are not reliable as an interconnect technology, the band pass filters require coplanar waveguide transmission line (CPW-TL) topologies.

With one metallic strip for the signal line and two large metallizations for the ground plane, the CPW-TL is the ideal choice for the microwave circuits that need both series and parallel connection of components without substrate vias [2].

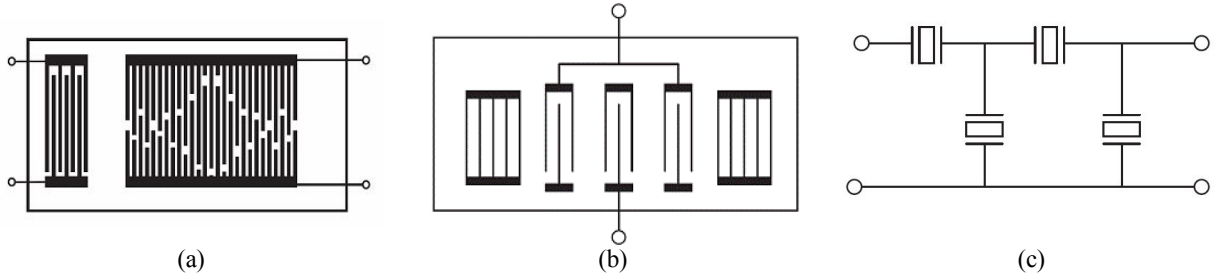


Fig.1. SAW based band-pass filters include: (a) delay line type filters; (b) longitudinally-coupled resonator filters; (c) impedance element filters (ladder filters)

The coupled resonator filters are difficult to implement in CPW-TL topology, while the delay line filters show high propagation losses for GaN/Si substrates. This was tested experimentally using test structures with face-to-face resonators with digit/interdigit of 200 nm, 150 nm and 130 nm. Typical results are shown in Fig.2 where, for a distance between the resonators of only 600 μm , the propagation losses are 36 dB, 46.7 dB, 49.6 dB for 5.44 GHz, 7 GHz, 8 GHz, respectively. This led to the choice of the impedance element filter (IEF) configuration.

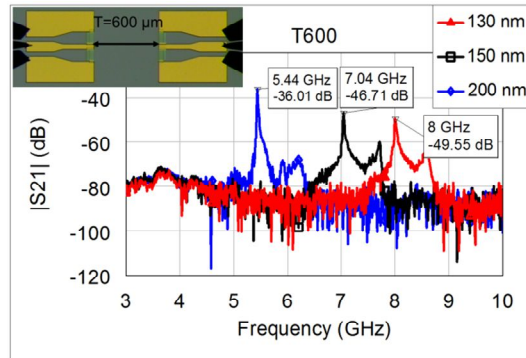


Fig. 2. Transmission parameter of SAW test structures with digit/interdigit of 130 nm, 150 nm and 200 nm

Two basic topologies are of choice for the IEF: (1) PI type configuration (Fig. 3 (a)) and (2) T-type configuration (Fig. 3 (b)). The general theory for the IEF design requires the fulfillment of the following conditions for the SAW resonators (Fig. 4):

$$\begin{aligned}
 f_{s,SAW_H} &= f_0 \\
 f_{p,SAW_H} &= f_{c2} > f_0 \\
 f_{p,SAW_V} &= f_0 \\
 f_{s,SAW_V} &= f_{c1} < f_0
 \end{aligned} \tag{1}$$

where f_0 is the filter central operating frequency, f_s is the series resonance frequency and f_p is the parallel resonance frequency of the SAW-R, f_{c1} is the lower maximum rejection frequency and f_{c2} is the higher maximum rejection frequency.

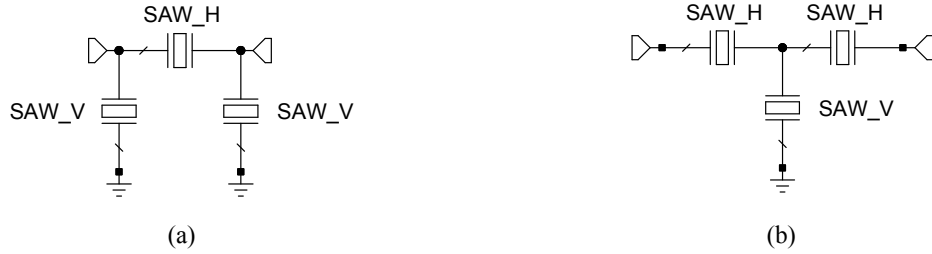


Fig. 3 BPF topologies for the final filter design: (a) PI-type configuration; (b) T-type configuration

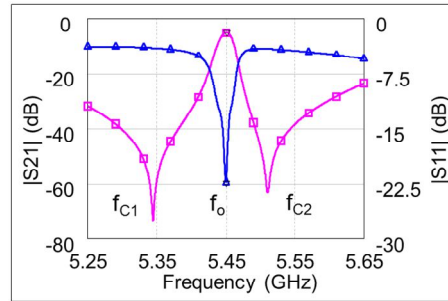


Fig. 4. Band pass filter characteristic and the definition of the central frequency and the rejection frequencies

This approach requires a strict control of the series and parallel resonance frequencies of the SAW-Rs. The effective coupling coefficient of the SAW processed on GaN/Si is limited to a maximum value of 0.3%, which leads to a difference between the two resonance frequencies of few MHz.

III. FABRICATION PROCESS FOR SUB-MICRON INTERDIGITAL TRANSDUCERS

The fabrication of SAW-R based filters operating at frequencies higher than 3 GHz is not at all trivial. The IDT requires finger widths smaller than 300 nm and therefore advanced nanolithography and lift-off techniques that severely limit the thickness of the metallization. At the same time, in an effort to limit conductive losses, thicker metallization should be used for the connecting pads, CPW-TL, inductive components, etc.

The technological process was adapted to combine the thin metallization of the IDT with the thicker metal for the surrounding CPW-TL and components, while ensuring a good contact between the two areas. Thus, a three step fabrication process was developed (Fig. 5 (a)-(c)). First, the CPW-TL, pads, printed inductors and alignment marks are fabricated by means of classical photolithography and deposition of 5 nm titanium adherence layer and 150 nm gold layer. The second fabrication step is dedicated to the nanolithographic processing of the SAW-Rs by electron beam lithography (EBL), followed by the deposition of the thin metallization (Ti/Au – 5/95nm). A third processing step is employed in order to deposit an overlay metallization on the CPW and over the SAW-R contacts (Ti/Au – 5/150nm). This step ensures that any ruptures that might have occurred when depositing the 100 nm thin SAW-R metallization over the 150 nm CPW-TL are covered, thus providing good contact and overall thicker metallization for the CPW-TL areas (in total ~300 nm).

The e-beam lithography was performed in a dedicated EBL machine - Raith e-Line, using as electron resist PMMA 950k A4. Because of the charging effects due to the high resistivity of the GaN layer, the writing field for the IDTs was limited to a maximum of 100x100 μm^2 . Fig.6 (a) – (c) presents SEM images of interdigitated structures, fabricated using this process, with digit/interdigit spacings of 130 nm, 150 nm and 200nm. The metal layers were deposited using a highly directional e-beam evaporation equipment (Temescal FC 2000) in order to favor the lift-off process and to ensure a good quality of the deposited metal traces – neat lines without side walls.

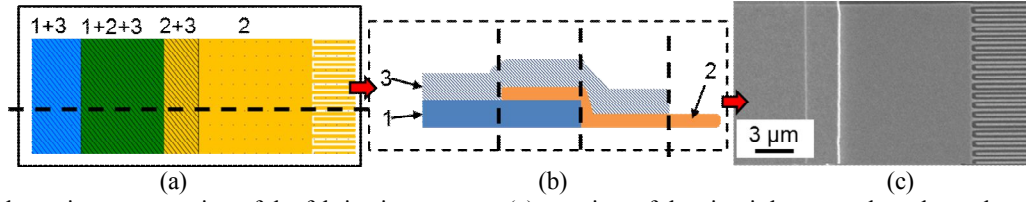


Fig.5. Schematic representation of the fabrication process: (a) top view of the circuit layout and mask number; (b) cross-section of the structure in the thin-metal/thick-metal contact area; (c) SEM image of the fabricated contact area

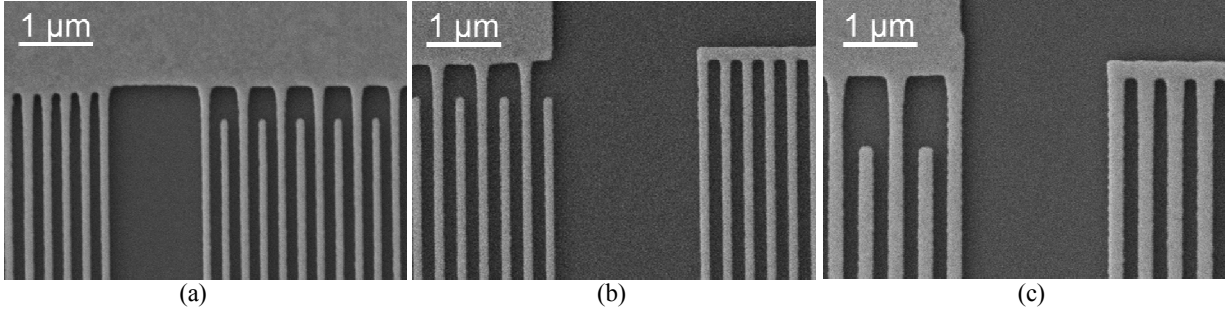


Fig.6. SEM images of interdigitated structures with different digit/interdigit spacings: (a) 130 nm; (b) 150 nm and (c) 200 nm

IV. SAW RESONATOR MODELING

The performance of the filter is determined by the individual SAW-Rs it consists of. Therefore, the study of the individual SAW-R is very important. Fig.7 presents an overview of a SAW-R with the definition of the main parameters. This model was used in COMSOL Multiphysics to investigate the behavior of the SAW-R.

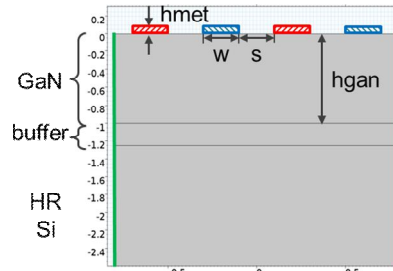


Fig. 7. Cross-section of a SAW-R

Starting from the constitutive equations (2) the solution of this equation system depends on the 3D/2D geometry of the structure, boundary conditions (in both mechanical and electrical domains) and on the material parameters.

$$\begin{aligned}
 T &= c_E S - e^T E \\
 D &= e S + \epsilon_S E
 \end{aligned}
 \tag{2}$$

The solution of the equation system can be represented in the form of the equivalent circuit model presented in Fig.8 (modified Butterworth Van-Dyke equivalent circuit of the SAW resonator). The branch with C_m - R_m - L_m models the piezoelectric effect, the coupling between the electromagnetic energy and the electromechanic energy. C_o is the static capacitance of the IDT, R_s is the series resistance of the electrodes and R_o models the dielectric losses in the GaN layer. The ratio C_m/C_o represents the effective coupling coefficient of the SAW-R.

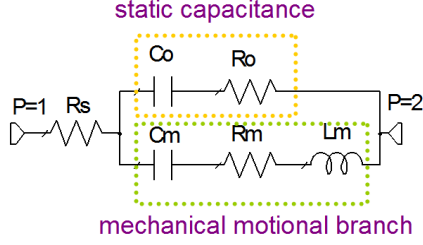


Fig.8. Modified Butterworth Van-Dyke equivalent circuit of the SAW resonator

If the losses are neglected, the equivalent impedance (Z) of the SAW resonator is given by (3).

$$Z = \frac{j\omega L_m \left(1 - \frac{\omega_s^2}{\omega^2}\right)}{(1 + L_m C_0 \omega_s^2) \left(\frac{\omega^2}{\omega_p^2} - 1\right)} \quad (3)$$

$$\omega_s^2 = \frac{1}{C_m L_m}$$

$$\omega_p^2 = \left(1 + \frac{C_m}{C_0}\right) \omega_s^2$$

where ω_s is the series resonance frequency and ω_p is the parallel resonance frequency.

For $w=s=200$ nm the series resonance frequency is about 5.5 GHz. Numerical simulations confirmed by experimental results showed that it is very difficult to accurately control the series and the parallel resonance frequencies by means of the IDT digit width, aspect ratio or metallization thickness [3]. The change in $w=s$ from 200 nm to 206 nm will decrease the resonance frequency with 151 MHz (approx. 25 MHz/nm) and an increase of 10 nm in the metallization thickness h_{met} will decrease the resonance frequency with 63 MHz (6.3 MHz/nm). According to [4] the simulated control rate is 5 MHz/nm for the electrode thickness and 0.7 MHz/nm for the electrode width (but for a constant $w+s$). The ratio C_m/C_0 is as low as 0.08% and the difference between the two resonance frequencies is less than 5 MHz. As a result it is not possible to obtain the frequency response from Fig.4 using the control of neither h_{met} nor the digit width/space.

V. LUMPED INDUCTOR SAW RESONATOR

The proposed approach is represented by printed series and parallel inductors to control the series and parallel resonance frequencies. In the case of series inductors a study is presented in [5]. A photo of the SAW-R tuned with a printed inductor is shown in Fig. 9 (a). A SEM detail of the IDT and part of the reflector is presented in the inset. The equivalent circuit schematic of the SAW-R with connecting pad and series inductor is shown in Fig. 9 (b). The equivalent impedance of the SAW-R with no electrical and mechanical losses is given by (3). Connecting this impedance in series with L_{ser} and solving for the zero reactance, equation (4) is obtained. The solutions of this equation are given by (5) for the approximation $L_{ser} \ll L_m$. The analytical solution for the series resonance frequency reveals two solutions (5) and the possibility of the control of series resonance by the series inductance.

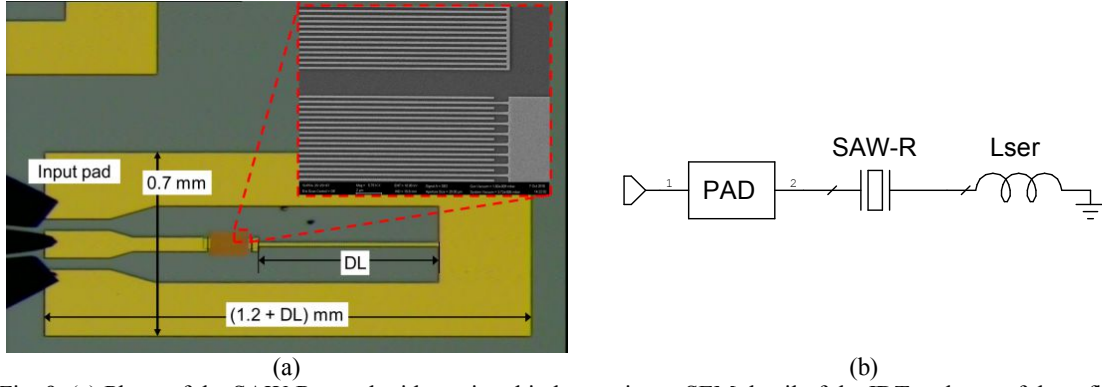


Fig. 9. (a) Photo of the SAW-R tuned with a printed inductor; inset: SEM detail of the IDT and part of the reflector; (b) equivalent circuit schematic of the SAW-R with connecting pad and series inductor (© 2017 IEEE. Reprinted, with permission, from [5])

The effect of the series inductor (L_{ser}) on the series resonance frequency (f_s - defined as the minimum value of the impedance magnitude - $|Z|$) is presented in Fig. 10 (a) and (b). The parallel resonant frequency (f_p - maximum value of $|Z|$) is practically unaffected. On the other hand, f_s is tuned towards lower frequencies for L_{ser} values up to 0.7 nH and becomes greater than f_p for higher values of L_{ser} . The tuning effect ($\Delta f/f_{ser}$) is of about 1% for all three pitch values for the considered inductance values (0.4 nH, 0.7 nH and 1.3 nH). The simulations are in very good agreement with measured results (Fig. 10 (b)), showing a tuning effect of about 0.75%.

$$\omega^4 + \left(\frac{1}{L_s C_0} - \omega_p^2\right) \omega^2 - \frac{\omega_p^2}{L_{ser} C_0} = 0 \quad (4)$$

$$(\omega'_s)^2 \approx \frac{\left(\omega_p^2 - \frac{1}{L_s C_0}\right) \pm \sqrt{\left(\frac{1}{L_s C_0} - \omega_p^2\right)^2 + 4 \frac{\omega_p^2}{L_s C_0}}}{2} \quad (5)$$

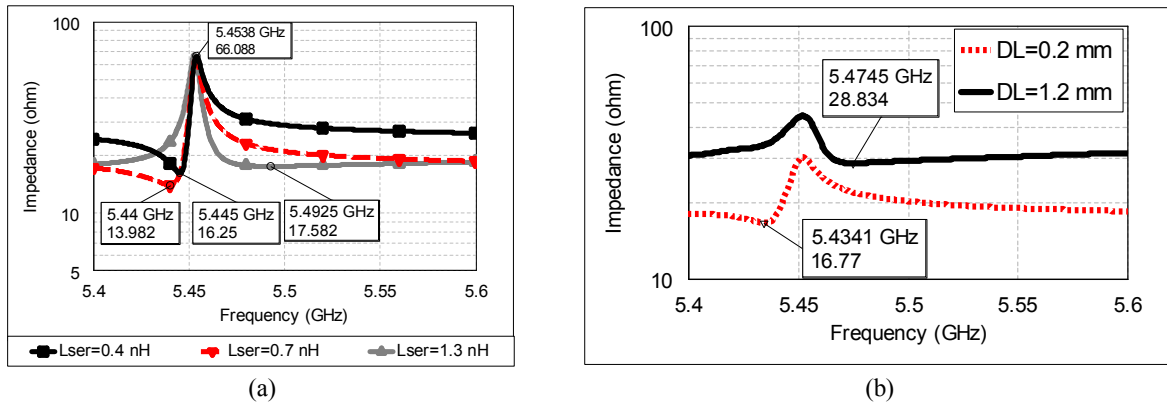


Fig. 10. Study of the effect of the series inductor (L_{ser}) on the resonance frequencies for pitch 0.4 μm : (a) simulation results; (b) measurement results (© 2017 IEEE. Reprinted, with permission, from [5])

Fig. 11 presents the S-parameter measurement results for the three SAW-R structures (pitch 0.4 μm , 0.3 μm and 0.26 μm) and the three values for DL (0.2 mm, 0.7 mm and 1.2 mm). The change in slope of the $|S_{11}|$ parameter vs frequency for DL=1.2 mm can be noticed. This is due to the fact that the monolithic integrated resonator (SAW-R placed in series with the printed inductor) changes its behavior from capacitive to inductive. An effective coupling coefficient of about 1% was measured for DL = 1.2 mm for all three pitches of the SAW-R structures.

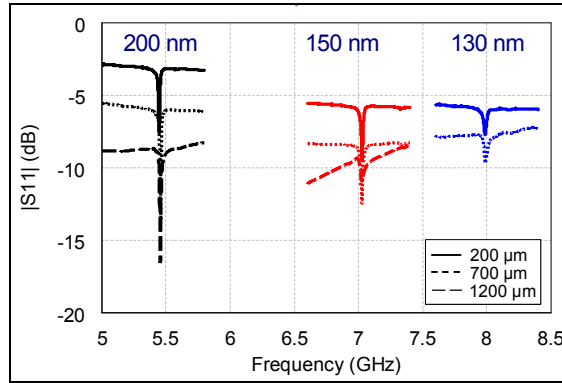


Fig. 11. S-parameter measurement results for the test structures (© 2017 IEEE. Reprinted, with permission, from [5])

The measured resonance frequency as a function of temperature was used to calculate the temperature coefficient of frequency (TCF) parameter [6]. Table I summarizes the experimental results obtained for the 293 K - 423 K temperature range, for the three values of DL and the three values of the pitch. The TCF values show only a slight dependence on DL and the pitch value. Therefore, there is no limitation for the filter design regarding the TCF, because the monolithically integrated resonators have the same temperature drift.

Table I. Summary of Temperature Dependence (© 2017 IEEE. Reprinted, with permission, from [5])

Pitch	DL = 0.2 mm		DL = 0.7 mm		DL = 1.2 mm	
	fres @ 293 K [GHz]	TCF [ppm]	fres @ 293 K [GHz]	TCF [ppm]	fres @ 293 K [GHz]	TCF [ppm]
0.4 μm	5.4485	NA	5.4585	-43.72	5.4565	-43.25
0.3 μm	7.0285	-41.66	7.0265	-40.47	7.0255	-39.88
0.26 μm	7.9865	-43.23	7.9895	-42.7	NA	NA

VI. TECHNOLOGICAL DISPERSION EFFECTS

Recently [4] and [7] presented the experimental investigation results of the technological dispersion effect on the resonance frequency of surface acoustic wave resonators (SAW-R) fabricated on GaN/Si. The dispersion investigations were performed on a processed quarter of a 3 inch wafer with 10 identical chips. The wafer was purchased from NTT Advanced Technology Corporation from Japan on custom request. The structure shown in Fig. 9 (a) was characterized on wafer using a Vector Network Analyzer system from Anritsu. The selected configuration (Fig. 12 (a) and (b)) was the following: an IDT with 100 digits with 200 nm width/space of the digit and 75 μm digit length with two reflectors placed on either side of the IDT. The reflectors consist of 60 digits each, are connected at both ends and are placed at a distance of 2 microns from the IDT. The length of the printed inductor is 1.2 mm.

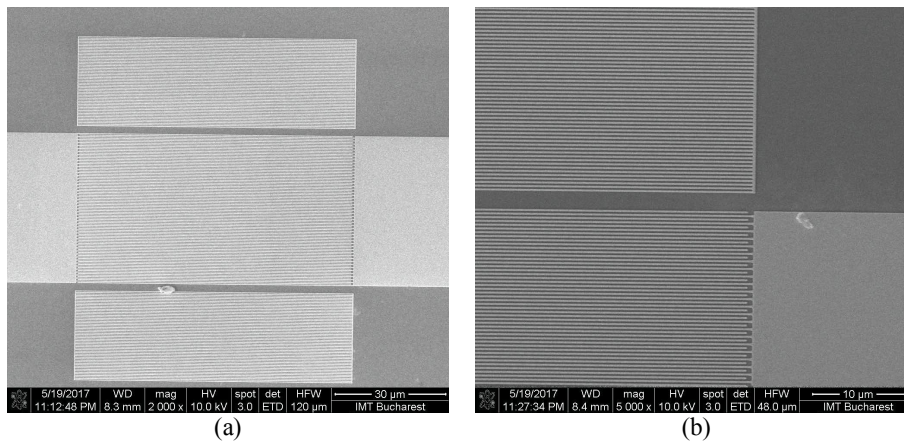


Fig. 12. SEM images: (a) the SAW-R test structure; (b) details of digits and reflectors

The deviation of the resonance frequency of the S11 parameter from the mean value, as a function of the distance to the center of the wafer for the 10 identical test structures, shows a maximum resonance frequency at a distance of about 15 mm. This value decreases towards the edge of the wafer quarter. The total frequency difference is about 98 MHz for a total distance of 30 mm from the center.

An investigation of the effect of the main technological parameters was performed using numerical modeling of the SAW-R in COMSOL Multiphysics. The main technological parameters that can influence the resonance frequency of the SAW-R (GaN layer thickness, IDT metallization thickness, electrode width, variation of the elastic constants due to the thermal strain) were varied around their nominal values. The summary of the variation rate is presented in Table II. This rate is compared to the expected deviation of the resonant frequency based on structural characterization results (SEM, AFM, ellipsometry).

Table II. Summary of simulated influence of technological parameters on the resonance frequency of the resonator and comparison with measurement results

Parameter	Variation rate	Expected deviation based on structural characterization results
GaN layer thickness	0.48 MHz/nm	10.5 MHz
Metal layer thickness	5 MHz/nm	25 MHz
Digit width	0.7 MHz/nm	7 MHz
Thermal strain	17.5 MHz/1%	N.A.

Even when considering the combination of the worst case scenario for the GaN layer thickness, metal layer thickness and digit width variation, the total frequency deviation doesn't fully account for the measured results (98 MHz). The only parameter which has a strong enough influence is the thermal strain, which for an induced variation of only 4% of the elastic coefficients gives a frequency deviation of 70 MHz. Furthermore, the variation of the thermal strain, together with the compensation techniques for minimum bowing of the wafer, offer an explanation for the maximum positive deviation which occurs at a distance of about 15 mm from the center of the wafer.

VII. SAW BAND PASS FILTER DESIGN

For the final filter design, the PI topology (Fig. 13 (a)) demonstrated the best performances as a SAW BPF. It consists of a horizontal branch with a SAW-R placed in parallel (BPF_AH) with the inductor L_{par} and two vertical branches with the SAW-Rs placed in series (BPF_AV) with inductor L_{ser} . The SAW-Rs consist of an IDT with digit/interdigit width of 200 nm. The area of the SAW-Rs was an optimization variable. For the final design the selected SAW-Rs are: BPF_AV with 200 digits of 50 μm length and BPF_AH with 170 digits of 100 μm length. The corresponding static capacitance values are $C_{oV} = 0.46$ pF and $C_{oH} = 0.76$ pF. After a first estimation of L_{ser} and L_{par} using analytical equations, their final values are obtained through circuit optimization. The values are $L_{par}=0.71$ nH and $L_{ser}=1.83$ nH.

The optimized filter response is presented in Fig. 13 (b). The insertion losses are about 10.4 dB at 5.5 GHz, the rejection is better than 40 dB at 5.42 GHz and 5.58 GHz, and the 3 dB bandwidth is 8 MHz.

The SAW-Rs also have losses (mechanical – R_m , conductive – R_s , dielectric – R_o) that affect the filter parameters. The effect of these losses is further evidenced in Table. III and in Fig. 14 (a) and (b). The insertion losses ($|S_{21}|_{max}$) depend strongly on the mechanical losses (R_m) and only slightly on the dielectric (R_o) and conductive (R_s) losses. At the same time, the mechanical losses do not affect the out of band rejection. This parameter is greatly damaged by the increase of the conductive and dielectric losses, at almost the same rate.

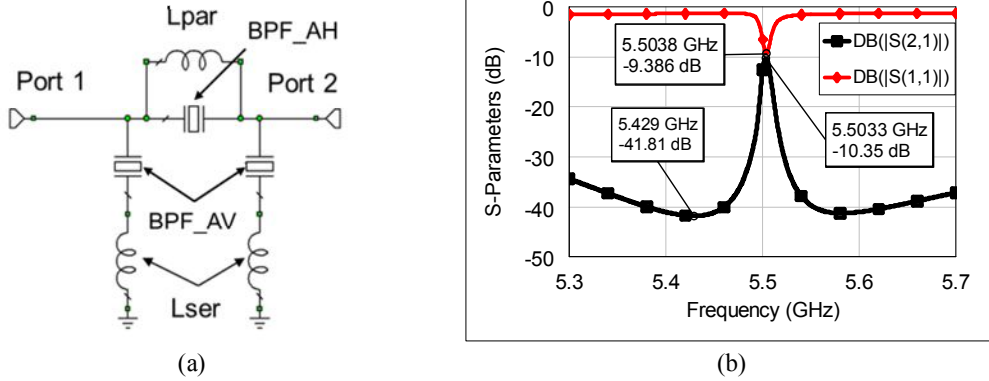


Fig. 13. (a) SAW filter topology; (b) optimized filter characteristics

Table III. Filter performances for different losses levels

	R_o [Ω]	R_s [Ω]	R_m [Ω]	$ S_{21} _{max}$ [dB]	Rejection [dB]
Optimized filter response	2	2	80	10.4	40
Var. 1	2	5	80	9.8	33
Var. 2	5	5	80	9.6	28
Var. 3	2	2	100	12.4	41
Var. 4	2	5	100	11.7	33

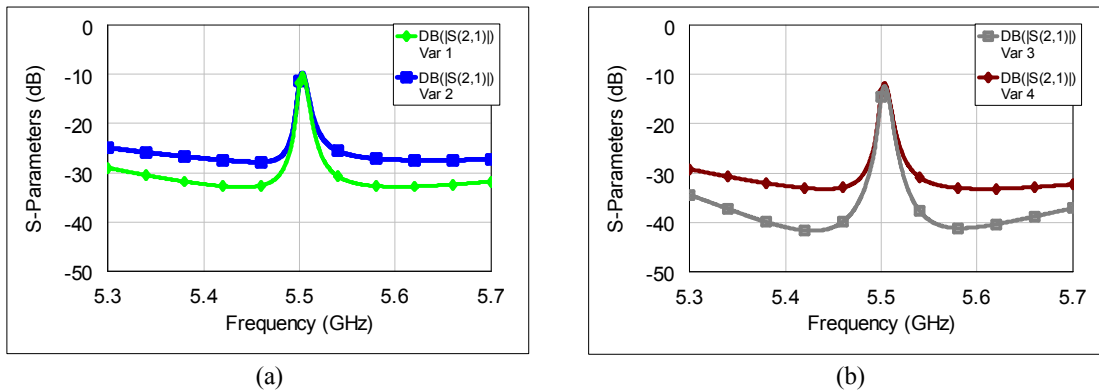


Fig. 14. Transmission parameter for different simulation scenarios (see. Table III): (a) Var. 1 and var. 2; (b) Var. 3 and Var. 4

VIII. CONCLUSION

A new approach, which uses printed inductors connected in series or in parallel with the SAW-R for the accurate control of the series and parallel resonance frequencies was presented. At frequencies higher than 5 GHz, these inductors are in the 0.2-2 nH range and can be integrated monolithically into the SAW-R based filter structure, resulting in a very compact device. Printed inductors with values between 0.2-1 nH were placed in series with SAW-Rs with IDT digit/interdigit widths within the 130-200 nm range, operating in the 5.4 - 8.6 GHz frequency range. Test structures were designed and processed on a semi-insulating 1 μm thin epitaxial GaN layer, using advanced nanolithographic techniques. It was shown that the printed inductors tuned the series resonance frequencies with up to 0.75% leading to the development of a PI-configuration band-pass filter based on the impedance element approach. A moderate temperature coefficient (about -40 ppm/K) was measured for the test structures with printed inductors.

The dispersion of the resonance frequency across a quarter of a 3" wafer was investigated and compared to the influence of the main technological parameters (GaN layer thickness, metallization thickness, electrode width, variation

of the elastic constants due to the thermal strain). The results indicate a main contribution of the variation of the thermal strain, together with the compensation techniques for minimum bowing of the wafer, to the frequency deviation (98 MHz).

A SAW-BPF design based on monolithic integration of printed inductors with SAW-Rs was proposed and circuit level simulation results were shown (insertion losses of 10.4 dB at 5.5 GHz, rejection better than 40 dB and 3 dB bandwidth of 8 MHz). It was shown that the insertion losses are mainly influenced by the mechanical losses and only slightly by the dielectric and conductive losses. The out of band rejection is mainly affected by the increase of the conductive and dielectric losses.

The main experimental results will be presented during the conference.

ACKNOWLEDGEMENTS

This work was supported by the European Space Agency (Contract No. 40000115202/ 15/NL/CBi).

REFERENCES

- [1]. K.Hashimoto, *Surface Acoustic Wave Devices in Telecommunications*, Springer-Verlag 2000
- [2]. I.Wolf, *Coplanar microwave integrated circuits*, 1st ed., Verlagsbuchhandlung, 2006
- [3]. A. Müller et al, "Nanoprocessing and Micromachining Technologies of GaN/Si for Sensors and Filters Operating at Frequencies above 5 GHz", *ESA SPCD 2016*
- [4]. A.C. Bunea, A.M. Dinescu, L.A. Farhat, C. Părvulescu, D. Neculoiu, "Effect of Key Technological Parameters on GaN/Si SAW Resonators Operating Above 5 GHz", *Romanian Journal of Information Science and Technology*, vol. 20, No. 4, 2017, pp. 354-368
- [5]. A. C. Bunea, D. Neculoiu and A. Dinescu, "GaN/Si monolithic SAW lumped element resonator for C- and X-band applications", *2017 IEEE Asia Pacific Microwave Conference (APMC)*, Kuala Lumpur, 2017, pp. 1010-1013.
- [6]. K.-Y. Hashimoto, M. Kadota, T. Nakao, M. Ueda, M. Miura, H. Nakamura, H. Nakanishi, K. Suzuki, "Recent development of temperature compensated SAW Devices," in *Proc. IEEE Int. Ultrason. Symp.*, Oct. 2011, pp. 79–86.
- [7]. A. C. Bunea, A. M. Dinescu, C. Părvulescu and D. Neculoiu, "Investigation of technological dispersion of GaN on silicon SAW resonators for bandpass filter applications", *2017 International Semiconductor Conference (CAS)*, Sinaia, 2017, pp. 123-126